Table 4
Characteristics and typical appearance of cirrhotic nodules at MR imaging

		Signal Intensity		Dynamic MR Imaging[a]	Kupffer Cell Density	SPIO[b]	Hepatocellular Function	Gd-EOB-DTPA[c]
		T1WI	T2WI					
RNs		Iso–Hyper (siderotic nodules; T1/T2WI, hypo)	Iso–Hypo	Iso–Hyper	Similar[d]	Iso[d]	Similar[d]	Iso[d]
DNs	Low grade	Hypo–Hyper	Hypo	Iso–Hyper	Various[d]	Hypo–Hyper[d]	Various[d]	Hypo–Hyper[d]
	High grade		Hypo–Slightly hyper					

Abbreviations: DNs, dysplastic nodules; Gd-EOB-DTPA, gadoxetic acid; Hypo, hypointense; Hyper, hyperintense; Iso, isointense; RNs, regenerative nodules; SPIO, superparamagnetic iron oxide.

[a] T1-weighted GRE image on delayed phase after administration of gadolinium-based contrast agents.

[b] T2-weighted GRE image after administration of SPIO.

[c] T1-weighted GRE image on hepatocyte-selective phase after administration of Gd-EOB-DTPA.

[d] Appearance is described in comparison with the surrounding hepatic parenchyma.

Data from Refs.[47–55,59–61]

elastography in an independent population of 35 healthy individuals and 48 patients with varying degrees of chronic liver disease showed a sensitivity of 86% and specificity of 85% for the detection of stages 2 to 4 fibrosis compared with liver histology from biopsy. A high negative predictive value (97%) for excluding the presence of fibrosis was also noted, suggesting that MR elastography might have a role in improving the ability to risk-stratify patients for liver biopsy to exclude occult advanced fibrosis.[39] MR elastography therefore appears to shows promise for the noninvasive staging of liver fibrosis, particularly in patients with advanced fibrosis.

Diffusion-weighted magnetic resonance imaging is a technique that assesses the freedom of diffusion of water protons within tissue by applying motion-sensitizing gradients that cause diffusing protons to lose signal. Recent advances in MR imaging technology have facilitated the performance of diffusion-weighted MR imaging of the liver, and it has also been used to detect liver fibrosis. Prior studies have reported that apparent diffusion coefficient (ADC) values acquired from b values of 500 (seconds/mm^2) and greater correlated significantly with liver fibrosis stage, and that ADC values with a combination of b value of 0 and 1000 (seconds/mm^2) showed the highest correlation ($r = -0.654$, $P<.001$).[40] On the other hand, several studies noted that there was no significant correlation between fibrosis stage and the ADC value using low b values (b values, 50 to 400 seconds/mm^2), because diffusion-weighted imaging with a low b value was influenced by perfusion contamination.[40,41] Luciani and colleagues,[42] reported that ADC calculated from low b values was significantly reduced in cirrhosis. Thus, the fast component diffusion-weighted MR imaging

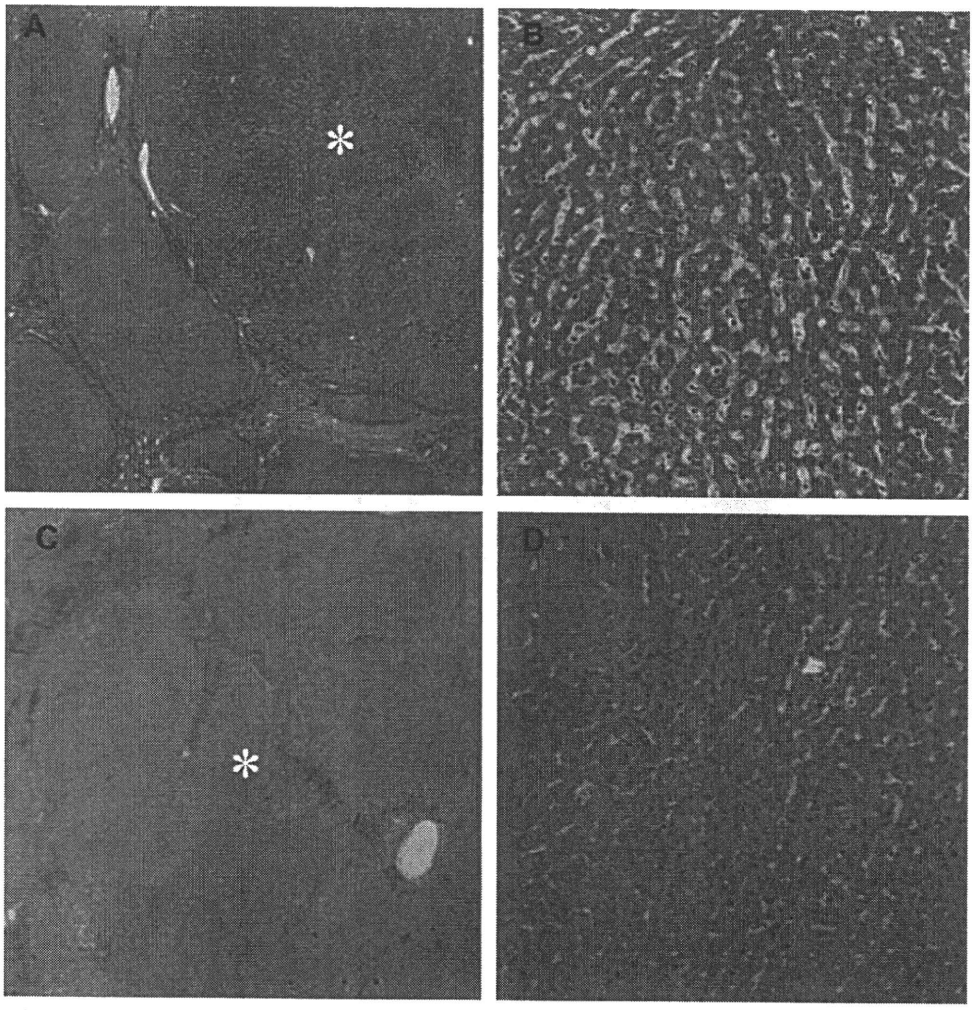

Fig. 16. Photomicrographs (Azan-Mallory stain, original magnification ×20 and ×100) in a patient with HCV shows low-grade dysplastic nodule (*asterisk*) (*A*, *B*) and high-grade dysplastic nodule (*asterisk*) (*C*, *D*). (*Courtesy of* Osamu Nakashima, MD, Department of Pathology, Kurume University School of Medicine, Japan.)

obtained with low b values may provide information related to microperfusion changes in diffuse liver disease whereas the slow component diffusion-weighted MR imaging obtained with high b values has been suggested to reflect a decrease in water proton diffusion.[43] The principles of diffusion-weighted MR imaging is discussed further in this presentation on functional MR imaging techniques.

In vivo MR spectroscopy (MRS) is most commonly used to assess signals from hydrogen (^{1}H) and phosphorus (^{31}P). Although ^{1}H-based MRS allows for the quantification of certain metabolites and lipids, ^{31}P-based MRS provides insights on processes, including cell turnover and energy state, based on the substantial ^{31}P concentrations within hepatocytes.[44] Previous studies have suggested MRS may be useful in detecting hepatic fibrosis.[45,46] An increased levels of hepatic phosphomonoesters (PME) have been reported in patients with established cirrhosis,[45,46] and an increasing PME to phosphodiester (PDE) ratio has been reported to correlate with worsening necroinflammatory and fibrosis scores on liver histology.[47] It has also been suggested that a PME and PDE ratio 0.2 or less is correlated with mild hepatitis and 0.3 or greater is correlated with cirrhosis in a study involving patients with chronic hepatitis C.[48] Despite some preliminary promising data, ^{31}P-based MRS is not widely used due to specific technical requirements. The role of MRS in the detection of liver inflammation and fibrosis requires further investigation.

CIRRHOSIS-ASSOCIATED HEPATOCELLULAR NODULES

Regenerative Nodules

Regenerative nodules form in response to necrosis, altered circulation, or other stimuli,[49] and may progress along a well-described carcinogenetic pathway to become dysplastic nodules or hepatocellular carcinomas.[50] These nodules are present in all cirrhotic livers and are surrounded by fibrous septa (see **Fig. 10**).[16] The nodules may be monoacinar or multiacinar, depending on

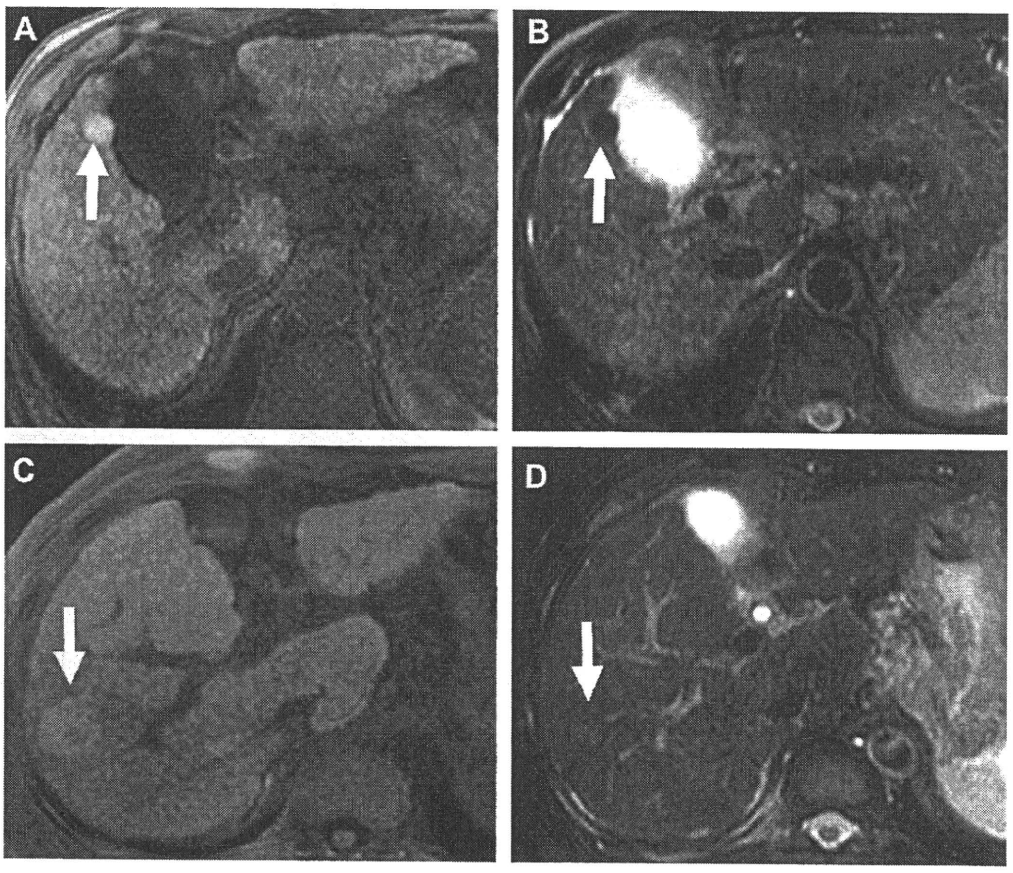

Fig. 17. Low-grade (*A, B*) and high-grade dysplastic nodules (*C, D*). All nodules were hyperintense on T1-weighted fat-saturated 3D GRE images (TR/TE = 3.6/1.7 ms, flip angle = 15°) (*A, C*) (*arrows*). In T2-weighted fat-saturated TSE images, in contrast, a low-grade dysplastic nodule is observed as hypointense (*B*) (*arrow*), whereas a high-grade nodule is observed as slightly hyperintense (*D*) (*arrow*).

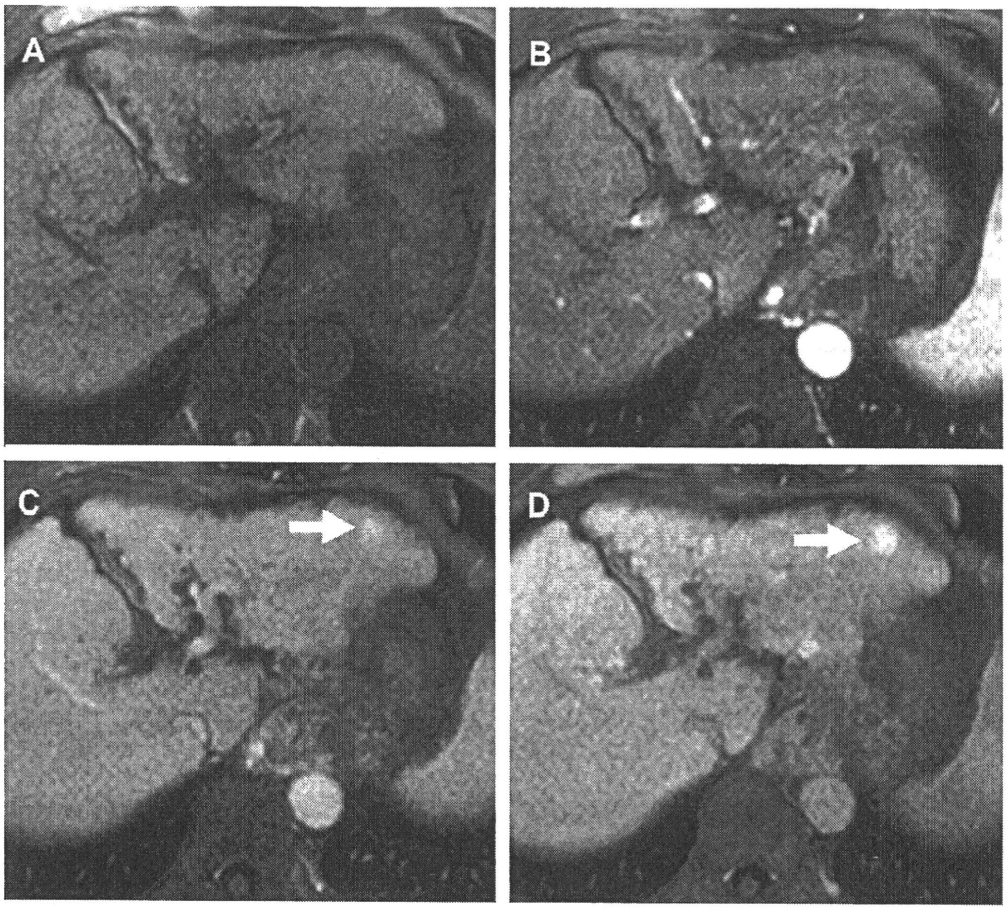

Fig. 18. Dynamic enhancement patterns of a high-grade dysplastic nodule in axial T1-weighted fat-saturated 3D GRE images (TR/TE = 3.6/1.7 ms, flip angle = 15°), presenting before (*A*) and in the arterial phase (30 s) (*B*), portal phase (90 s), and (*C*) equilibrium phase (4 min), and (*D*) after intravenous injection of Gd-EOB-DTPA. Portal and equilibrium phases (*arrow*) show increased enhancement of high-grade dysplastic nodule.

whether they contain one or more terminal portal tracts, and can also be classified by size as of the micronodular (≤3 mm) (**Fig. 14**), macronodular (>3 mm) (see **Fig. 14**), or mixed type (features of both micro- and macronodular types).[51]

MR imaging demonstrates regenerative nodules with greater sensitivity than any other imaging modality. These nodules usually appear isointense to hypointense (**Fig. 15**) on T2-weighted images relative to the surrounding inflammatory fibrous septa, and isointense to hyperintense (see **Fig. 15**) relative to background liver parenchyma on T1-weighted images.[52] The accumulation of iron within regenerative nodules (siderotic nodules) may cause hypointensity on both T1- and T2-weighted images (see **Fig. 15**) owing to susceptibility effects.[53] With regard to blood supply on dynamic imaging, regenerative nodules are usually enhanced to the same or greater degree than the background liver in the portal venous phase,[54] owing to the large contribution from the portal vein, with minimal contribution from the hepatic artery (**Table 4**).[55]

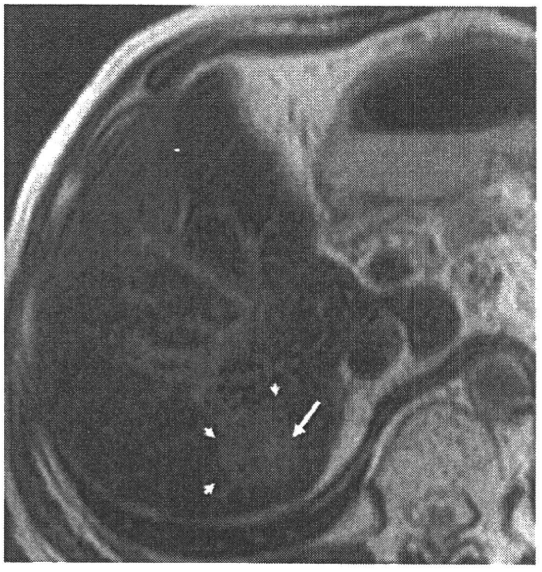

Fig. 19. T2-weighted TSE image shows an iso- to slightly high-signal–intensity nodule (*arrowheads*) with a focus of higher signal intensity (*arrow*) within the nodule. This higher signal intensity focus within the nodule shows the presence of HCC.

Dysplastic Nodules

Dysplastic nodules are considered an intermediate, premalignant step along the hepatocarcinogenesis process, and can also be classified by the degree of dysplasia as low- or high-grade.[56]

Low-grade dysplastic nodules are sometimes vaguely nodular but are often distinct from the surrounding cirrhotic liver because of the presence of peripheral fibrous scar.[56] This nodule is not a true capsule, but rather condensation of scarring as is seen around all cirrhotic nodules. Low-grade dysplastic nodules show mild increase in cell density with a uniform pattern, and without cytologic atypia.[56] Architectural changes beyond clearly regenerative features are not present; these lesions do not contain pseudoglands or markedly thickened trabeculae (**Fig. 16**).[56] High-grade dysplastic nodules may also be distinctly or vaguely nodular in the background of cirrhosis, although they also lack a true capsule, similar to low-grade dysplastic nodules; however, they are more likely to show a vaguely nodular pattern than low-grade dysplastic nodules.[56] A high-grade dysplastic nodule is defined as having architectural and/or cytologic atypia, but the atypia is insufficient for a diagnosis of HCC.[56] These lesions most often show increased cell density, sometimes more than 2 times higher than the surrounding nontumoral liver, often with an irregular trabecular pattern (see **Fig. 16**).[56] On MR imaging, dysplastic nodules have variable

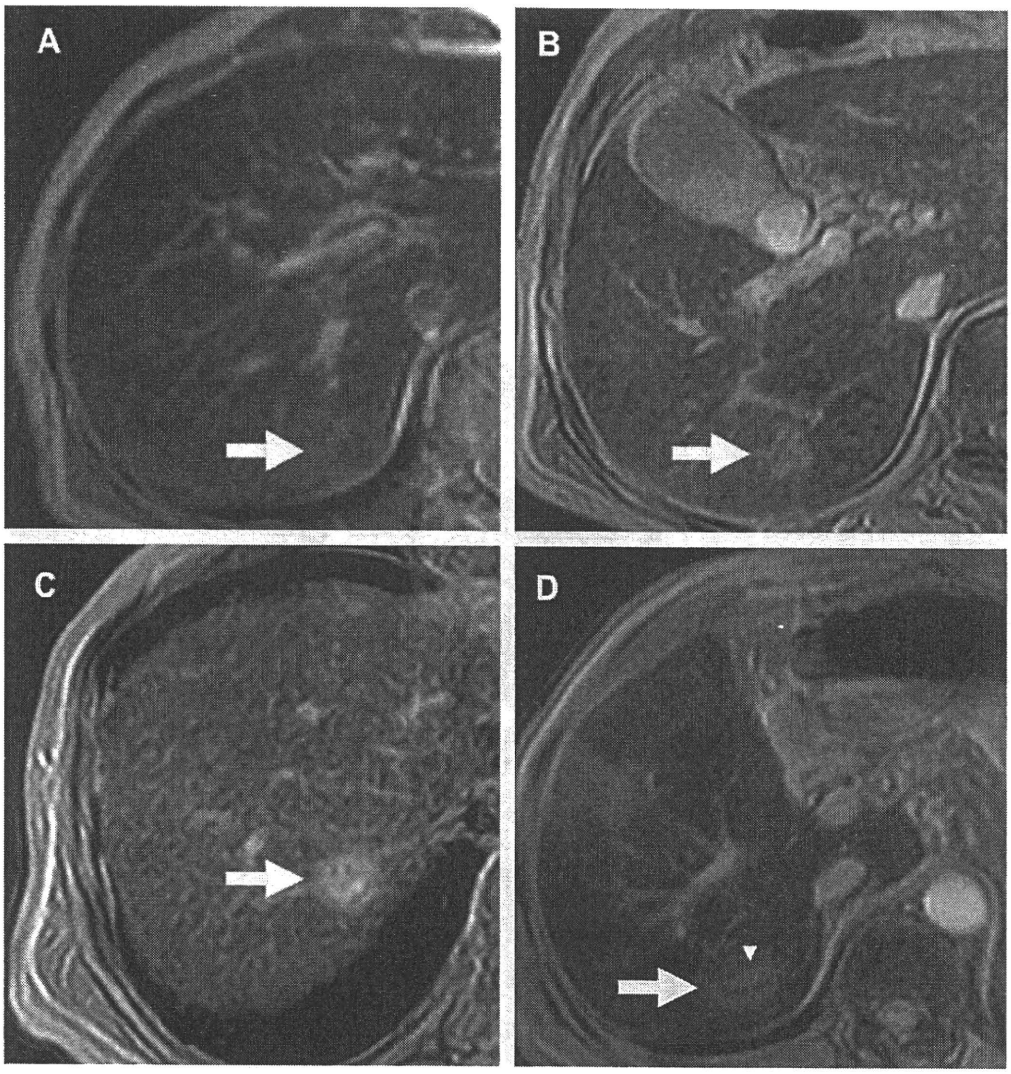

Fig. 20. T2-weighted GRE images (TE, 9.5 ms) after administration of SPIO in well-differentiated hepatocellular carcinoma (HCC) shows various signal intensities depending on Kupffer cell function within the nodule (*A–D*) (*arrow*). A dysplastic nodule with a central focus of HCC is observed as "a nodule within a nodule" (*D*) (*arrowhead*).

appearances, and their signal intensity characteristics overlap with those of regenerative nodules and well-differentiated HCC. On T2-weighted images, most dysplastic nodules are usually hypointense, and only rarely hyperintense (**Fig. 17**) It has been suggested that high-grade dysplastic nodules tend to have slightly higher signal intensity on T2-weighted images (see **Fig. 17**)[57]; however, the distinction from HCC and a high-grade dysplastic nodule may be difficult even on pathology. On T1-weighted images dysplastic nodules characteristically demonstrate high signal intensity, which may be related to deposition of copper, Fe^{3+}, or glycogen, or a high protein or lipid content (see **Fig. 17**).[58,59] However, the appearance on T1-weighted images cannot be used to distinguish low- and high-grade dysplastic nodules because both display variable (low, iso-, or high) signal intensity.[57]

With regard to blood supply, dysplastic nodules are typically hypovascular lesions with predominantly portal venous blood supply, although increased arterial flow is seen in a small minority of cases (**Fig. 18**) (see **Table 4**).[60] The signal intensity characteristics of some high-grade dysplastic nodules that receive increasing supply from the hepatic artery may overlap with those of HCC nodules during the process of hepatocarcinogenesis.[61] The hepatocarcinogenesis theory has been supported by the description of a dysplastic nodule with a central focus of HCC on T2-weighted images as "a nodule within a nodule."[62] The classic MR appearance is a focus of high signal intensity within a low-signal–intensity nodule on T2-weighted images (**Fig. 19**). This focus of HCC may also be enhanced in the arterial phase.[63] Despite the possibility of HCC developing within dysplastic nodules, the development of this tumor may not be a linear process because HCC is recognized to occur in patients with chronic HBV but without cirrhosis.

Liver-Specific MR Contrast Agents (SPIO, Gd-EOB-DTPA) for Liver Nodules

Because the density of Kupffer cells within regenerative nodules is similar to that in the surrounding nonneoplastic hepatic parenchyma, these nodules take up SPIO through Kupffer cell phagocytosis. On T2-weighted GRE and T2-weighted spin-echo sequences after administration of SPIO, regenerative nodules show the same signal intensity as that of surrounding hepatic parenchyma. In contrast, because Kupffer cell density within

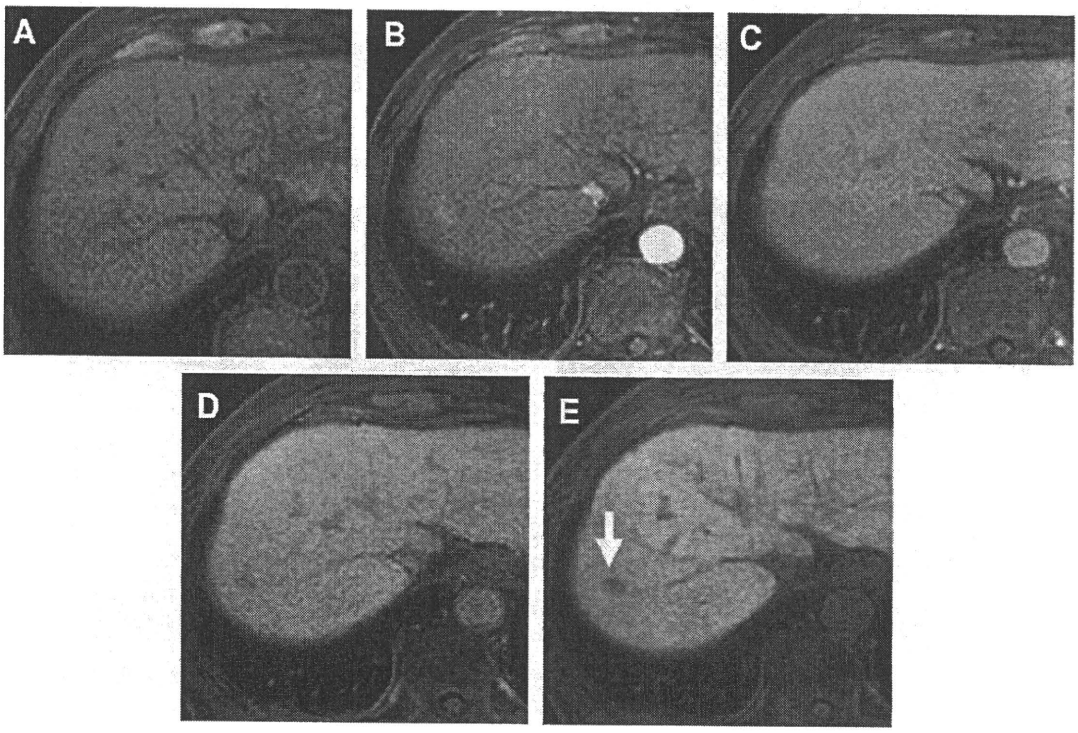

Fig. 21. Dynamic enhancement patterns of well-differentiated HCC in axial 3D fat-saturated T1-weighted GRE images (TR/TE = 3.6/1.7 ms, flip angle = 15°), presenting before (*A*) and in the arterial phase (*B*), portal phase (*C*), equilibrium phase (*D*), and hepatocyte-selective phase (*E*) after intravenous injection of Gd-EOB-DTPA. Well-differentiated HCC is commonly observed as hypointense in the hepatocyte-selective phase (*arrow*).

dysplastic nodules and well-differentiated HCC is variable, the signal intensity of these nodules may also vary after administration of SPIO.[57,64] It has been suggested that the extent of SPIO uptake may reflect the degree of Kupffer cell function (**Fig. 20**).[65] Signal intensity characteristics of dysplastic nodules after administration of SPIO also overlap with those of regenerative nodules and well-differentiated HCC, and uptake of SPIO into these nodules may cause a decrease in detection.

Regenerative nodules generally have normal hepatocellular function and therefore demonstrate uptake of hepatocellular contrast agents such as Gd-EOB-DTPA. As dedifferentiation proceeds, the number of expressed organic anion transporters decreases, with a resulting progressive decrease in the uptake of hepatocellular agents.[66] It is considered that the appearance of HCC at hepatocyte-selective phases with hepatocellular agents is dependent on the degree of tumor differentiation. However, hepatocytes in well-differentiated HCC may retain enough hepatocellular function to take up hepatocellular agents, and hence may be overlooked at this phase of imaging, or appear similar to a regenerative or dysplastic nodule (see **Table 4**).

In the authors' experience, most well-differentiated HCCs diagnosed by needle biopsy are clearly observed as hypointense to liver at hepatocyte-selective phases on Gd-EOB-DTPA–enhanced MR imaging (**Fig. 21**). Nevertheless, some well-differentiated HCCs are observed as isointense or hyperintense. Conclusive differentiation of dysplastic nodules from well-differentiated HCCs appears difficult (**Fig. 22**). Moreover, the diagnostic differentiation of dysplastic nodules from other cirrhosis-associated hepatocellular nodules may be difficult even on histopathologic analysis, and the use of molecular genetics-based techniques may be necessary in future.[61]

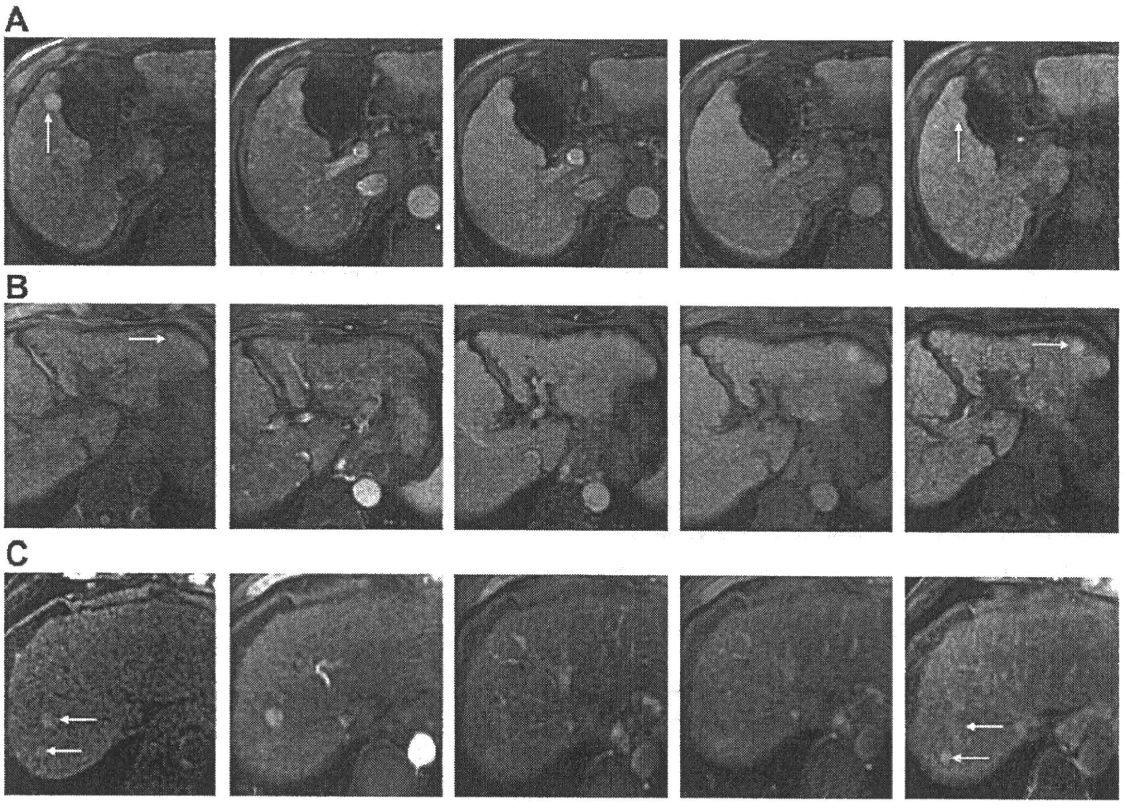

Fig. 22. Dynamic enhancement patterns of a low-grade dysplastic nodule (*A*), high-grade dysplastic nodule (*B*), and well-differentiated HCCs (*C*) in axial T1-weighted fat-saturated 3D GRE images (TR/TE = 3.6/1.7 ms, flip angle = 15°), presenting before and in the arterial phase, portal phase, equilibrium phase, and hepatocyte-selective phase after intravenous injection of Gd-EOB-DTPA. In the hepatocyte-selective phase, each nodule is observed as isointense or hyperintense owing to the uptake of hepatocellular agents (*arrows*). In series (*C*), both nodules were well-differentiated HCCs. In the hepatocyte-selective phase, both HCCs are observed as isointense and hyperintense, respectively. All these HCCs were diagnosed by needle biopsy.

REFERENCES

1. Mortele KJ, Ros PR. MR imaging in chronic hepatitis and cirrhosis. Semin Ultrasound CT MR 2002;23(1): 79–100.
2. Popper H. Pathologic aspects of cirrhosis. A review. Am J Pathol 1978;87:228–58.
3. Garcia-Tsao G, Lim JK. Members of Veterans Affairs Hepatitis C Resource Center Program. Management and treatment of patients with cirrhosis and portal hypertension: recommendations from the Department of Veterans Affairs Hepatitis C Resource Center Program and the National Hepatitis C Program. Am J Gastroenterol 2009;104(7):1802–29.
4. Sorrell MF, Belongia EA, Costa J, et al. National Institutes of Health Consensus Development Conference Statement: management of hepatitis B. Ann Intern Med 2009;150:104–10.
5. Global surveillance and control of hepatitis C. Report of a who consultation organized in collaboration with the viral hepatitis prevention board, Antwerp, Belgium. J Viral Hepat 1999;6:35–47.
6. Davis GL, Albright JE, Cook SF, et al. Projecting future complications of chronic hepatitis C in the United States. Liver Transpl 2003;9:331–8.
7. Afdhal NH. The natural history of hepatitis C. Semin Liver Dis 2004;24(Suppl 2):3–8.
8. Maher JJ. Alcoholic liver disease. In: Feldman M, Friedman LS, Sleisenger MH, editors. Gastrointestinal and liver disease, vol. II. Philadelphia: Saunders; 2002. p. 1375–91.
9. Breitkopf K, Nagy LE, Beier JI, et al. Current experimental perspectives on the clinical progression of alcoholic liver disease. Alcohol Clin Exp Res 2009; 33:1647–55.
10. Greenfield V, Cheung O, Sanyal AJ. Recent advances in nonalcoholic fatty liver disease. Curr Opin Gastroenterol 2008;24(3):320–7.
11. Itoh H, Sakai T, Takahashi N, et al. Periportal high intensity on T2-weighted MR images in acute viral hepatitis. J Comput Assist Tomogr 1992;16:564–7.
12. Matsui O, Kadoya M, Takashima T, et al. Intrahepatic periportal abnormal intensity on MR images: an indication of various hepatobiliary diseases. Radiology 1989;171:335–8.
13. Fisher MR, Gore RM. Computed tomography in the evaluation of cirrhosis and portal hypertension. J Clin Gastroenterol 1985;7:173–81.
14. Ito K, Mitchell DG, Gabata T. Enlargement of hilar periportal space: a sign of early cirrhosis at MR imaging. J Magn Reson Imaging 2000;11:136–40.
15. Ito K, Mitchell DG. Imaging diagnosis of cirrhosis and chronic hepatitis. Intervirology 2004;47:134–43.
16. Ito K, Mitchell DG, Siegelman ES. Cirrhosis: MR imaging features. Magn Reson Imaging Clin N Am 2002;10:75–92.
17. Lafortune M, Matricardi L, Denys A, et al. Segment 4 (the quadrate lobe): a barometer of cirrhotic liver disease at US. Radiology 1998;206:157–60.
18. Ito K, Mitchell DG, Gabata T, et al. Expanded gallbladder fossa: simple MR imaging sign of cirrhosis. Radiology 1999;211:723–6.
19. Ito K, Mitchell DG, Kim MJ, et al. Right posterior hepatic notch sign: a simple diagnostic MR finding of cirrhosis. J Magn Reson Imaging 2003;18:561–6.
20. Okazaki H, Ito K, Fujita T, et al. Discrimination of alcoholic from virus-cirrhosis on MR imaging. AJR Am J Roentgenol 2000;175:1677–81.
21. Ito K, Mitchell DG, Outwater EK, et al. Primary sclerosing cholangitis: MR imaging features. AJR Am J Roentgenol 1999;172(6):1527–33.
22. Brancatelli G, Federle MP, Ambrosini R. Cirrhosis: CT and MR imaging evaluation. Eur J Radiol 2007; 61(1):57–69.
23. Wenzel JS, Donohoe A, Ford KL 3rd, et al. Primary biliary cirrhosis: MR imaging findings and description of MR imaging periportal halo sign. AJR Am J Roentgenol 2001;176:885–9.
24. Kobayashi S, Matsui O, Gabata T, et al. MRI findings of primary biliary cirrhosis: correlation with Scheuer histologic staging. Abdom Imaging 2005;30(1): 71–6.
25. Martí-Bonmatí L. MR contrast agents in hepatic cirrhosis and chronic hepatitis. Semin Ultrasound CT MR 2002;23(1):101–13.
26. Vilgrain V. Ultrasound of diffuse liver disease and portal hypertension. Eur Radiol 2001;11:1563–77.
27. Van Beers BE, Leconte I, Materne R, et al. Hepatic perfusion parameters in chronic liver disease: dynamic CT measurements correlated with disease severity. AJR Am J Roentgenol 2001;176:667–73.
28. Semelka RC, Chung JJ, Hussain SM, et al. Chronic hepatitis: correlation of early patchy and late linear enhancement patterns on gadolinium-enhanced MR images with histopathology: initial experience. J Magn Reson Imaging 2001;13:385–91.
29. Faria SC, Ganesan K, Mwangi I, et al. MR imaging of liver fibrosis: current state of the art. Radiographics 2009;29(6):1615–35.
30. Yeh MM, Brunt EM. Pathology of nonalcoholic fatty liver disease. Am J Clin Pathol 2007;128(5):837–47.
31. Bedossa P, Dargere D, Paradis V. Sampling variability of liver fibrosis in chronic hepatitis C. Hepatology 2003;38:1449–57.
32. Bici NC, Semelka RC. Contrast agents for MR imaging of the liver. Radiol Clin North Am 2005; 43(5):887–98.
33. Lucidarme O, Baleston F, Cadi M, et al. Non-invasive detection of liver fibrosis: Is superparamagnetic iron oxide particle-enhanced MR imaging a contributive technique? Eur Radiol 2003;13(3):467–74.
34. Aguirre DA, Behling CA, Alpert E, et al. Liver fibrosis: noninvasive diagnosis with double contrast

material-enhanced MR imaging. Radiology 2006; 239:425–37.
35. Martí-Bonmatí L, Lonjedo E, Poyatos C, et al. MnDPDP enhancement characteristics and differentiation between cirrhotic and noncirrhotic livers. Invest Radiol 1998;33(10):717–22.
36. Murakami T, Baron RL, Federle MP, et al. Cirrhosis of the liver: MR imaging with mangafodipir trisodium (Mn-DPDP). Radiology 1996;198(2):567–72.
37. Muthupillai R, Lomas DJ, Rossman PJ, et al. Magnetic resonance elastography by direct visualization of propagating acoustic strain waves. Science 1995;269:1854–7.
38. Muthupillai R, Ehman RL. Magnetic resonance elastography. Nat Med 1996;2:601–3.
39. Yin M, Talwalkar JA, Glaser KJ, et al. Assessment of hepatic fibrosis with magnetic resonance elastography. Clin Gastroenterol Hepatol 2007;5(10): 1207–13.
40. Taouli B, Tolia AJ, Losada M, et al. Diffusion-weighted MRI for quantification of liver fibrosis: preliminary experience. AJR Am J Roentgenol 2007;189:799–806.
41. Boulanger Y, Amara M, Lepanto L, et al. Diffusion-weighted MR imaging of the liver of hepatitis C patients. NMR Biomed 2003;16:132–6.
42. Luciani A, Vignaud A, Cavet M, et al. Liver cirrhosis: intravoxel incoherent motion MR imaging—pilot study. Radiology 2008;249:891–9.
43. Koinuma M, Ohashi I, Hanafusa K, et al. Apparent diffusion coefficient measurements with diffusion-weighted magnetic resonance imaging for evaluation of hepatic fibrosis. J Magn Reson Imaging 2005;22:80–8.
44. Jalan R, Taylor-Robinson SD, Hodgson HJF. In vivo hepatic magnetic resonance spectroscopy: clinical or research tool? J Hepatol 1999;25:414–24.
45. Khan SA, Cox IJ, Hamilton G, et al. In vivo and in vitro nuclear magnetic resonance spectroscopy as a tool for investigating hepatobiliary disease: a review of H and P MRS applications. Liver Int 2005;25:273–81.
46. Munakata T, Griffiths RD, Martin PA, et al. An in vivo ^{31}P MRS study of patients with liver cirrhosis: progress towards a non-invasive assessment of disease severity. NMR Biomed 1993;6:168–72.
47. Van Wassenaer-van Hall HN, van der Grond J, van Hattum J, et al. ^{31}P magnetic resonance spectroscopy of the liver: correlation with standardized serum, clinical, and histological changes in diffuse liver disease. Hepatology 1995;21:443–9.
48. Menon DK, Sargentoni J, Taylor-Robinson SD, et al. Effect of functional grade and etiology on in vivo hepatic phosphorus-31 magnetic resonance spectroscopy in cirrhosis: biochemical basis of spectral appearances. Hepatology 1995; 21:417–27.
49. Cho SG, Kim MY, Kim HJ, et al. Chronic hepatitis: in vivo proton MR spectroscopic evaluation of the liver and correlation with histopathologic findings. Radiology 2001;221:740–6.
50. Coleman WB. Mechanisms of human hepatocarcinogenesis. Curr Mol Med 2003;3(6):573–88.
51. Lee RG. Fibrosis and cirrhosis. In: Lee RG, editor. Diagnostic liver pathology. St Louis (MO): Mosby-Year Book, Inc; 1994. p. 281–308.
52. Krinsky GA, Lee VS. MR imaging of cirrhotic nodules. Abdom Imaging 2000;25:471–82.
53. Zhang J, Krinsky GA. Iron-containing nodules of cirrhosis. NMR Biomed 2004;17(7):459–64.
54. Seale MK, Catalano OA, Saini S, et al. Hepatobiliary-specific MR contrast agents: role in imaging the liver and biliary tree. Radiographics 2009;29(6): 1725–48.
55. Lim JH, Kim EY, Lee WJ, et al. Regenerative nodules in liver cirrhosis: findings at CT during arterial portography and CT hepatic arteriography with histopathologic correlation. Radiology 1999;210(2): 451–8.
56. International Consensus Group for Hepatocellular Neoplasia. Pathologic diagnosis of early hepatocellular carcinoma: a report of the international consensus group for hepatocellular neoplasia. Hepatology 2009;49(2):658–64.
57. Hanna RF, Aguirre DA, Kased N, et al. Cirrhosis-associated hepatocellular nodules: correlation of histopathologic and MR imaging features. Radiographics 2008;28(3):747–69.
58. Amano S, Ebara M, Yajima T, et al. Assessment of cancer cell differentiation in small hepatocellular carcinoma by computed tomography and magnetic resonance imaging. J Gastroenterol Hepatol 2003; 18:273–9.
59. Ebara M, Fukuda H, Kojima Y, et al. Small hepatocellular carcinoma: relationship of signal intensity to histopathologic findings and metal content of the tumor and surrounding hepatic parenchyma. Radiology 1999;210:81–8.
60. Matsui O, Kadoya M, Kameyama T, et al. Benign and malignant nodules in cirrhotic livers: distinction based on blood supply. Radiology 1991;178:493–7.
61. Willatt JM, Hussain HK, Adusumilli S, et al. MR Imaging of hepatocellular carcinoma in the cirrhotic liver: challenges and controversies. Radiology 2008; 247(2):311–30.
62. Mitchell DG, Rubin R, Siegelman ES, et al. Hepatocellular carcinoma within siderotic regenerative nodules: appearance as a nodule within a nodule on MR images. Radiology 1991;178(1):101–3.
63. Goshima S, Kanematsu M, Matsuo M, et al. Nodule-in-nodule appearance of hepatocellular carcinomas: comparison of gadolinium-enhanced and ferumoxides-enhanced magnetic resonance imaging. J Magn Reson Imaging 2004;20(2):250–5.

64. Lim JH, Choi D, Cho SK, et al. Conspicuity of hepatocellular nodular lesions in cirrhotic livers at ferumoxides-enhanced MR imaging: importance of Kupffer cell number. Radiology 2001;220(3):669–76.
65. Tonan T, Fujimoto K, Azuma S, et al. Evaluation of small (< or = 2 cm) dysplastic nodules and well-differentiated hepatocellular carcinomas with ferucarbotran-enhanced MRI in a 1.0-T MRI unit: utility of T2*-weighted gradient echo sequences with an intermediate-echo time. Eur J Radiol 2007; 64(1):133–9.
66. Gandi SN, Brown MA, Wong JG, et al. MR contrast agents for liver imaging: what, when, how. Radiographics 2006;26:1621–36.